

AN AUTOMATED FRAMEWORK FOR LARGE-SCALE GRAPH-BASED CEREBROVASCULAR ANALYSIS

Daniele Falcetta¹, Liane S. Canas², Lorenzo Suppa^{1,3}, Matteo Pentassuglia¹, Jon Cleary², Marc Modat², Sébastien Ourselin², Maria A. Zuluaga^{1,2}

¹ EURECOM, Sophia Antipolis, France

² School of Biomedical Engineering & Imaging Sciences, King’s College London, UK

³ Politecnico di Torino, Torino, Italy

ABSTRACT

We present *CaravelMetrics*, a computational framework for automated cerebrovascular analysis that models vessel morphology through skeletonization-derived graph representations. The framework integrates atlas-based regional parcellation, centerline extraction, and graph construction to compute fifteen morphometric, topological, fractal, and geometric features. The features can be estimated globally from the complete vascular network or regionally within arterial territories, enabling multiscale characterization of cerebrovascular organization. Applied to 570 3D TOF-MRA scans from the IXI dataset (ages 20–86), *CaravelMetrics* yields reproducible vessel graphs capturing age- and sex-related variations and education-associated increases in vascular complexity, consistent with findings reported in the literature. The framework provides a scalable and fully automated approach for quantitative cerebrovascular feature extraction, supporting normative modeling and population-level studies of vascular health and aging.

Index Terms— Vessel graphs, vascular features, vascular aging, neurovascular image analysis.

1. INTRODUCTION

Brain blood vessels change throughout the lifespan, with vessel density declining, curvature increasing, and branching patterns reorganizing, with implications for brain health [1]. Understanding cerebrovascular morphology is critical for detecting disease and distinguishing pathological from normal changes. To that end, population-level analyses are crucial as individual vessel measurements cannot be interpreted without demographic-specific reference ranges. These reference ranges allow discrimination between healthy aging and pathological changes across groups, and identification of clinical biomarkers that distinguish disease-related alterations from normal variations within the population. However, large-scale analyses have been limited by manual vessel tracing and a lack of automated biomarker extraction tools that can be used at scale.

Current approaches for cerebrovascular analysis can be classified into three categories. Segmentation-based methods, enabled by recent advances in deep learning for accurate automated vessel segmentation, typically from time-of-flight magnetic resonance angiography (TOF-MRA), estimate arterial volume from the segmented masks at the whole brain and regional levels [2]. Atlas-based approaches provide population references through statistical arterial atlases [3], offering normative cerebrovascular anatomy baselines. However, both approaches focus on simple volumetric and diameter measurements that may fail to completely characterize the vascular tree. Finally, graph-based computational tools use a segmentation mask as input to generate a graph representation of the vascular tree, from which intensity and morphometric features are extracted [4, 5, 6, 7, 8]. While commonly used, these tools are either semi-automatic [4, 7] or have been specifically designed for a particular type of image [5, 6, 8], limiting their usage at scale for any neurovascular imaging modality.

In this work, we present *CaravelMetrics*, an automated framework for analyzing the cerebrovascular tree. Our framework extracts fifteen morphometric, topological, fractal, and geometric vascular features from a graph generated from vascular binary masks, thus being agnostic to the underlying image modality. Similar to [2], we integrate an atlas of arterial regions, allowing us to analyze the cerebrovascular tree at both the whole-brain and regional levels. We showcase the potential of our open-source tool by analyzing the IXI Dataset¹, a cohort of 570 subjects aged 20 to 86 years whose cerebrovascular trees were imaged using TOF-MRA. Our analysis reveals that our features effectively capture variations in the vessels across a population.

2. METHODS

CaravelMetrics relies on representing the cerebrovascular network as a mathematical graph structure that is extracted from a vascular binary mask. The graph and the vascular binary mask are then used to extract morphometric, topological,

¹<https://brain-development.org/ixi-dataset/>

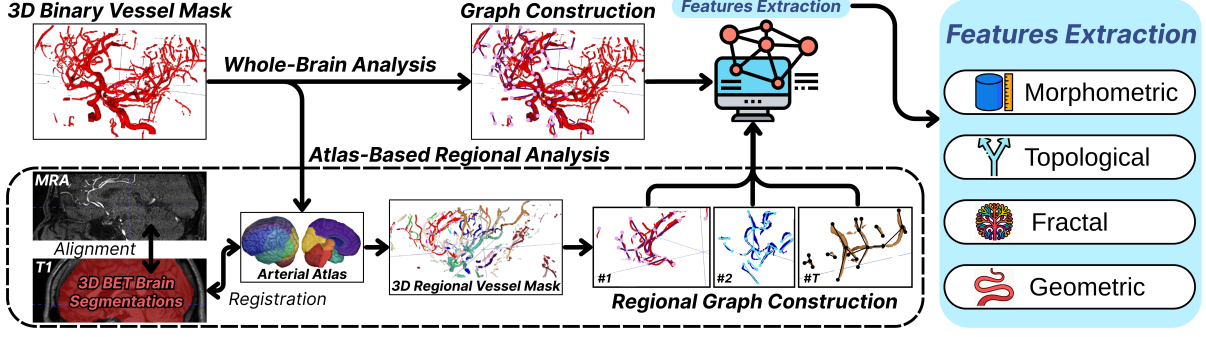


Fig. 1. Overview of the vascular feature extraction framework.

Table 1. List of vascular features extracted in within the vessel analysis framework.

Category	Metric	Definition/Formulation	Application
Morphometric	Total vessel length	$L = \sum_{(u,v) \in E} d_{uv}$	Structural integrity
	Volume	$ M \Delta x \Delta y \Delta z$	Vascular volume
Topological	Bifurcation count	$N_{bif} = \{v \in V : \deg(v) = 3\} $	Branching complexity
	Bifurcation density	N_{bif}/L	
	Number of loops	$ E_k - V_k + 1$	Connectivity patterns
	Loop lengths	$\sum_{(u,v) \in \text{loop}} d_{uv}$ for each loop	
Abnormal degree nodes	$ \{v \in V : \deg(v) > 3\} $	Anomalous branching	
Connected components	$ \{G_k\} $	Network integrity	
Fractal	Fractal dimension	$-\frac{\Delta \log(N(\epsilon))}{\Delta \log(\epsilon)}$; $N(\epsilon)$ the boxes at scale ϵ	Multi-scale organization
	Lacunarity	$\frac{\text{Var}(n)}{[\text{Mean}(n)]^2} + 1$; n the number of voxels per box	Spatial heterogeneity
Geometric	Geodesic length	$L_{geo}(P) = \sum_{i=1}^{n-1} d_{v_i v_{i+1}}$	Segment Arc Length
	Instantaneous curvature	$\kappa(t) = \frac{\ \mathbf{x}'(t) \times \mathbf{x}''(t)\ }{\ \mathbf{x}'(t)\ ^3}$ on interpolated $\mathbf{x}(t)$	Local geometry
	Mean curvature	$\bar{\kappa} = \frac{1}{L_{geo}} \int_0^1 \frac{\kappa(t)}{n(t)} \ \mathbf{x}'(t)\ dt$	Average tortuosity
	Mean square curvature	$\frac{1}{L_{geo}} \int_0^1 \frac{\kappa^2(t)}{[n(t)]^2} \ \mathbf{x}'(t)\ dt$	Curvature variability
	Arc-over-chord ratio	$L_{geo}(P) / \ \mathbf{x}_{v_1} - \mathbf{x}_{v_n}\ $	Segment tortuosity

fractal, and geometric features that can be aggregated at the whole-brain or regional level through the usage of an arterial atlas (Figure 1).

Graph Representation of Cerebrovascular Networks. Let us denote $M : \Omega \subset \mathbb{Z}^3 \rightarrow \{0, 1\}$, a binary vascular mask obtained from any 3D imaging modality. Given M , we define its skeleton $S = \text{Skel}(M) \subseteq \Omega$ as a one-voxel-thick subset that preserves the topological properties of M , such that $S \subseteq M$, $\text{conn}(S) = \text{conn}(M)$, and $\text{hom}(S) = \text{hom}(M)$, where $\text{conn}(\cdot)$ denotes the number of connected components and $\text{hom}(\cdot)$ describes the topology (loops and holes).

From the skeleton points $\mathbf{x} = (x, y, z) \in S \subset \mathbb{Z}^3$, we construct an undirected weighted graph $G = (V, E)$, where each skeleton point corresponds to a node $v \in V$ with spatial coordinates $\mathbf{x}_v \in \mathbb{Z}^3$. Edges $E = \{(u, v)\}$ connect pairs of nodes within a $3 \times 3 \times 3$ neighborhood (26-connectivity), with edge weights defined as the Euclidean distance $d_{uv} = \|u - v\|_2$.

A vascular graph G may consist of k disconnected sub-

graphs, each corresponding to an individual vessel component, such that $G = \bigsqcup_k G_k$. Within a given G_k , a root node serves as a reference point for segment extraction. We define three root nodes to ensure representative coverage of the vascular structure: R_1 corresponds to the end-point ($\deg(v) = 1$) with the largest vessel diameter, R_2 to the end-point with the second-largest diameter, and R_3 to the bifurcation node ($\deg(v) \geq 3$) with the largest diameter. If no bifurcation exists, R_3 defaults to R_1 . Based on this, a *vessel branch* or *segment* denotes the shortest path between a selected root node $s \in \{R_1, R_2, R_3\}$ and each reachable end-point $e \in V_{\text{end}}$ within the same G_k :

$$P_{s \rightarrow e} = \arg \min_{p \in \mathcal{P}(s, e)} \sum_{(u, v) \in p} d_{uv}, \quad (1)$$

where $\mathcal{P}(s, e)$ denotes the set of paths between s and e in G_k .

Feature Extraction. The framework extracts fifteen complementary vascular features grouped into four categories (Table 1), each capturing a distinct property of cerebrovas-

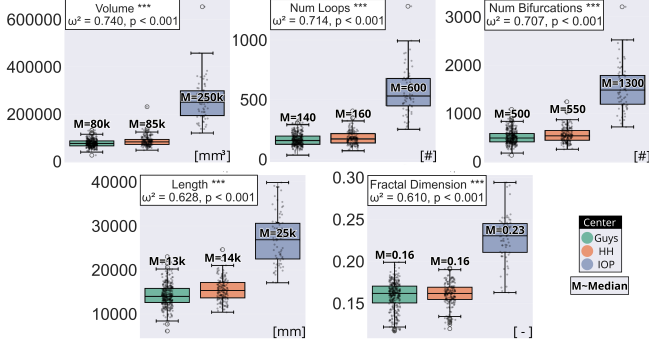


Fig. 2. Scanner-induced systematic bias. Consistent IOP shift across all features demonstrates acquisition artifacts.

cular organization. Morphometric features quantify network extent and capacity through total vessel length and volume. Topological features describe branching architecture and connectivity using bifurcation count, loop number, and component analysis. Fractal features characterize hierarchical self-similarity via box-counting and lacunarity [9]. Finally, geometric features quantify vessel tortuosity, reflecting arterial stiffening and age-related alterations, by capturing local vessel morphology and shape irregularity through cubic-spline parameterization of discrete centerline segments (Eq. 1) as continuous curves $\mathbf{x}(t) : [0, 1] \rightarrow \mathbb{R}^3$, with curvature values weighted by path multiplicity $n(t)$ and averaged across root nodes $s \in \{R_1, R_2, R_3\}$ to obtain descriptors for each G_k .

Atlas-Based Regional Analysis. The cerebrovascular tree exhibits heterogeneous patterns across brain territories, motivating a region-based analysis across arterial territories. We enable such analysis by aligning an arterial atlas $\mathcal{A} = \{T_i\}_{i=1}^T$, which partitions the brain into T arterial territories, with the original neurovascular image. This yields territory-specific masks defined as $M_i = M \cap T_i$. Our framework supports two complementary analysis modes: *whole-brain analysis*, performed on the complete graph $G = (V, E)$ derived from M ; and *region-specific analysis*, performed on regional graphs $G_i = (V_i, E_i)$ derived from each M_i . This formulation enables the extraction of vessel features globally or within anatomical arterial territories.

Implementation Details. Skeletonization, graph generation, and feature extraction are implemented in Python 3.10 with NumPy, SciPy, scikit-image, and NetworkX. We employ the open-source 3D brain MRI arterial territories atlas proposed in [10] ($T = 30$). Atlas-to-image alignment is done through multi-step registration: brain extraction via FSL BET [11], reorientation to MNI space, atlas to structural image registration using FLIRT with mutual information, and structural image to neurovascular image co-registration. Code and documentation are available in the project’s repository².

²<https://github.com/i-vesseg/CaravelMetrics>

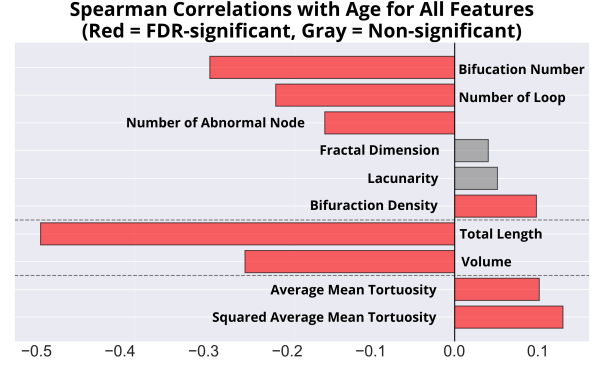


Fig. 3. Age effects on vessel morphometry. Significant age correlations (red bars) after FDR correction.

3. EXPERIMENTS & RESULTS

We demonstrate the relevance of the proposed framework by analyzing 570 healthy subjects, aged 20–86 years, from the IXI dataset, with multiple MR sequences acquired across three London hospitals with different scanners: Guy’s Hospital (Guys), Hammersmith Hospital (HH), and Institute of Psychiatry (IOP). Each subject has associated demographic information, including age, sex, height, weight, education, and occupation. We compute the body mass index (BMI) from the height and weight, and categorize individuals into 4 BMI-based groups according to standard clinical thresholds.

Using IXI’s TOF-MRA deep learning-generated binary vessel masks from the VesselVerse dataset [12], our aim is to use features from *CaravelMetrics* to quantify age-related cerebrovascular changes across the healthy adult lifespan and identify demographic factors associated with vessel morphology, tortuosity, and network topology, consistent with the literature (e.g., [13]). For the atlas-based regional analysis, we considered T1w MR images within IXI as structural images for multi-step registration. In our analysis, age associations employ Spearman correlations and one-way ANOVA across quartile-based groups with η^2 effect sizes. Demographic comparisons utilize t-tests for binary factors (sex) and one-way ANOVA for categorical variables (BMI, education), with ω^2 effect sizes for unbalanced groups. Multi-center effects undergo site-stratified analysis to separate biological variation from acquisition artifacts. All analyses apply Benjamini-Hochberg False Discovery Rate (FDR) correction ($q < 0.05$) to control for multiple comparisons.

Results. Initial analysis revealed substantial site effects, with IOP showing markedly different vessel distributions than Guys and HH (Figure 2), likely reflecting scanner/acquisition variations [3], though age imbalances may have contributed. Excluding IOP and focusing on the two homogeneous sites ($n = 488$) strengthened age effects: total vessel length effect size increased from $\eta^2 = 0.137$ to 0.204 (6.7 percentage

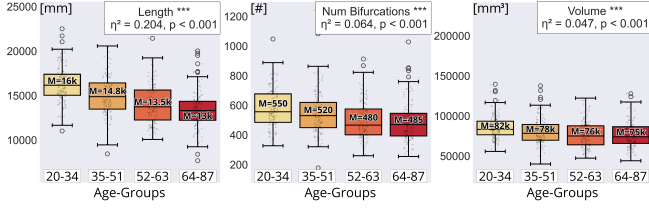


Fig. 4. Age-related vessel changes. Group differences across multiple morphometric and topological features.

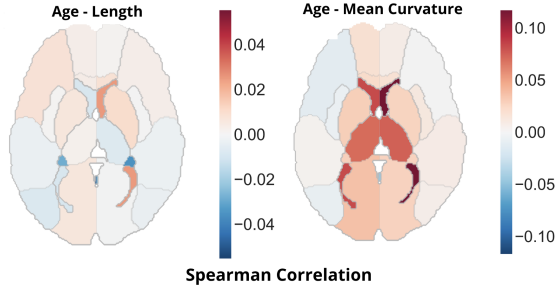


Fig. 5. Region-specific age effects. Vessel length (left) and curvature (right) correlations across 30 brain arterial regions.

points), suggesting site heterogeneity attenuates biological associations.

Analyzing age-related cerebrovascular changes, strong negative correlations emerged between age and structural vessel metrics across the adult lifespan (Figure 3), with total vessel length showing the most pronounced decline ($r = -0.50$, $p < 0.001$), corresponding to 20% reduction from youngest to oldest subjects (Figure 4). Volume ($r \approx -0.25$) and bifurcation count ($r \approx -0.25$) also declined significantly, reflecting network simplification. Conversely, bifurcation density and tortuosity increased with age ($r \approx +0.08$ and $+0.10$), consistent with arterial stiffening, while fractal dimension and lacunarity showed no significant correlations, indicating preserved topological scaling despite structural changes. Quartile-based age group analysis revealed large effect sizes: total length $\eta^2 = 0.204$, volume $\eta^2 = 0.047$, bifurcations $\eta^2 = 0.064$ (all $p < 0.001$). Regional analysis (Figure 5) revealed modest changes, with vessel length showing weak negative correlations in anterior territories and tortuosity increases in posterior and deep brain regions, though correlations remained relatively small across all territories. This pattern likely reflects measurement noise at smaller scales and the systemic nature of cerebrovascular aging, affecting the entire vascular network uniformly. Regarding anthropometric factors, normal-weight individuals ($n = 252$) demonstrated longer vessels than overweight ($n = 146$) or obese ($n = 55$) groups ($\eta^2 = 0.032$, $p = 0.007$; Figure 6, left). Height showed positive correlations with multiple vessel metrics ($\eta^2 = 0.026$ – 0.053), with taller individuals demonstrating higher bifurcation density, volume, and

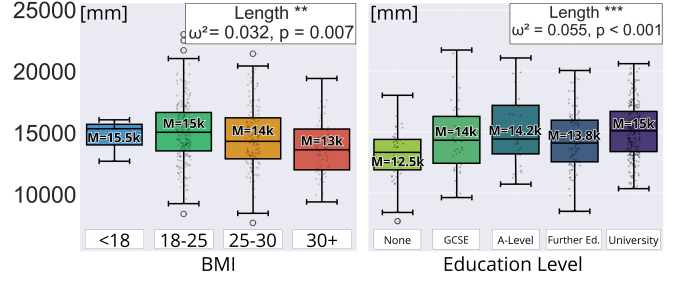


Fig. 6. Demographic effects on vessel length. BMI (left) and education (right) gradients.

network complexity, reflecting brain size scaling. Concerning sex, after IOP removal, males ($n = 223$) showed higher bifurcation density ($d = 0.384$), loops ($d = 0.321$), and volume ($d = 0.29$), along with lower lacunarity ($d = 0.193$), than females ($n = 265$), consistent with known neuroanatomical differences [13]. Finally, education analysis was prioritized over occupation given stronger age confounding in the latter (retired individuals averaged 68 years versus 26 for students), revealing a clear stepwise gradient in vessel length across qualification levels ($\eta^2 = 0.055$, $p < 0.001$; Figure 6, right), consistent with cognitive reserve extending to cerebrovascular architecture [14].

4. DISCUSSION AND CONCLUSION

We introduced *CaravelMetrics*, an automated framework for cerebrovascular characterization that extracts fifteen complementary features encompassing morphometric, topological, fractal, and geometric descriptors. By integrating an arterial atlas, the framework supports both whole-brain and territory-specific analyses, enabling multiscale assessment of cerebrovascular organization. As it operates directly on binary vessel masks, *CaravelMetrics* is compatible with diverse neurovascular imaging modalities. Applied to 570 subjects from the IXI dataset (ages 20–86), the framework revealed age-related declines in vessel length, volume, and bifurcation count, alongside increased tortuosity and education-associated increases in vessel length. These patterns are consistent with findings reported in the literature, supporting the validity of the proposed framework for cerebrovascular feature extraction and analysis at scale. A key limitation of our approach is its dependence on the quality of the deep learning-generated input masks. While we did not explicitly assess this, results suggest our framework is resilient to moderate segmentation noise. Future research should evaluate this robustness, develop strategies to address inaccuracies, and explore the framework’s applicability in more challenging pathological groups. *CaravelMetrics* enables reproducible, population-scale analysis of cerebrovascular networks that can help understand brain health and aging.

5. COMPLIANCE WITH ETHICAL STANDARDS

This study uses the publicly available datasets IXI and VesselVerse. No additional ethical approval was required.

6. ACKNOWLEDGMENTS

This work is co-funded by the European Union (EU) (ERC CARAVEL 101171357), and supported by France Life Imaging (ANR-11-INBS-0006). LSC acknowledges support from TwinsUK Imaging: A Resource for Ageing Research (Chronic Disease Research Foundation). MM and SO are supported by King's Health Partners Digital Health Hub and the EPSRC.

The authors have no competing interests to declare that are relevant to the content of this article. Views and opinions expressed are those of the authors only and do not necessarily reflect those of the EU or the ERC. Neither the EU nor the granting authority can be held responsible for them.

7. REFERENCES

- [1] H. C. Bennett, Q. Zhang, Y.-t. Wu, S. B. Manjila, U. Chon, D. Shin, D. J. Vanselow, H.-J. Pi, P. J. Drew, and Y. Kim, "Aging drives cerebrovascular network remodeling and functional changes in the mouse brain," *Nature communications*, vol. 15, no. 1, pp. 6398, 2024.
- [2] B. Guo, Y. Chen, J. Lin, B. Huang, X. Bai, C. Guo, B. Gao, Q. Gong, and X. Bai, "Self-supervised learning for accurately modelling hierarchical evolutionary patterns of cerebrovasculature," *Nature Communications*, vol. 15, no. 1, pp. 9235, 2024.
- [3] P. Mouches and N. D. Forkert, "A statistical atlas of cerebral arteries generated using multi-center MRA datasets from healthy subjects," *Scientific data*, vol. 6, no. 1, pp. 29, 2019.
- [4] L. Chen, M. Mossa-Basha, N. Balu, G. Canton, J. Sun, K. Pimentel, T. S. Hatsukami, J.-N. Hwang, and C. Yuan, "Development of a quantitative intracranial vascular features extraction tool on 3D MRA using semiautomated open-curve active contour vessel tracing," *Magnetic resonance in medicine*, vol. 79, no. 6, pp. 3229–3238, 2018.
- [5] P. Spangenberg, N. Hagemann, A. Squire, N. Förster, S. D. Krauß, Y. Qi, A. Mohamud Yusuf, J. Wang, A. Grüneboom, L. Kowitz, S. Korste, M. Totzeck, Z. Cibir, A. A. Tuz, V. Singh, D. Siemes, L. Struensee, D. R. Engel, P. Ludewig, L. Martins Nascentes Melo, I. Helfrich, J. Chen, M. Gunzer, D. M. Hermann, and A. Mosig, "Rapid and fully automated blood vasculature analysis in 3D light-sheet image volumes of different organs," *Cell Reports Methods*, vol. 3, no. 3, pp. 100436, 2023.
- [6] J. R. Bumgarner and R. J. Nelson, "Open-source analysis and visualization of segmented vasculature datasets with VesselVio," *Cell Reports Methods*, vol. 2, no. 4, pp. 100189, 2022.
- [7] R. Li, S. Chatterjee, Y. Jiaerken, X. Zhou, C. Radhakrishna, P. Benjamin, S. Nannoni, D. J. Tozer, H. S. Markus, and C. T. Rodgers, "LUMEN—A deep learning pipeline for analysis of the 3D morphology of the cerebral lenticulostriate arteries from time-of-flight 7T MRI," *NeuroImage*, vol. 318, pp. 121377, 2025.
- [8] G. Yang, X. Luo, J. Zhao, F. Fan, H. Li, B. Dong, L. Zhang, and Y. Zhang, "RVPD: An Automated System for Calculating the Tortuosity and Bifurcation Angles of Retinal Vessels to Predict Diseases," in *2025 IEEE 22nd International Symposium on Biomedical Imaging (ISBI)*. IEEE, 2025, pp. 1–5.
- [9] D. J. Gould, T. J. Vadakkan, R. A. Poché, and M. E. Dickinson, "Multifractal and lacunarity analysis of microvascular morphology and remodeling," *Microcirculation*, vol. 18, no. 2, pp. 136–151, 2011.
- [10] C.-F. Liu, J. Hsu, X. Xu, G. Kim, S. M. Sheppard, E. L. Meier, M. I. Miller, A. E. Hillis, and A. V. Faria, "Digital 3D brain MRI arterial territories atlas," *Scientific Data*, vol. 10, no. 1, pp. 74, 2023.
- [11] S. M. Smith, M. Jenkinson, M. W. Woolrich, C. F. Beckmann, T. E. J. Behrens, H. Johansen-Berg, P. R. Bannister, M. De Luca, I. Drobnjak, D. E. Flitney, R. K. Niazy, J. Saunders, J. Vickers, Y. Zhang, N. De Stefano, J. M. Brady, and P. M. Matthews, "Advances in functional and structural MR image analysis and implementation as FSL," *NeuroImage*, vol. 23, pp. S208–S219, 2004.
- [12] D. Falcetta, V. Marciano, K. Yang, J. Cleary, L. Legris, M. D. Rizzaro, I. Pitsiorlas, H. Chaptoukaev, B. Lemason, B. Menze, and M. A. Zuluaga, "VesselVerse: A Dataset and Collaborative Framework for Vessel Annotation," in *proceedings of Medical Image Computing and Computer Assisted Intervention – MICCAI 2025*, September 2025, vol. LNCS 15972.
- [13] M. E. H. Ophelders, M. J. A. Van Eldik, I. N. Vos, Y. S. Beentjes, B. K. Velthuis, and Y. M. Ruijgrok, "Anatomical differences of intracranial arteries according to sex: a systematic review and meta-analysis," *Journal of Neuroradiology*, vol. 51, no. 1, pp. 10–15, 2024.

- [14] Y. Stern, E. M. Arenaza-Urquijo, D. Bartrés-Faz, S. Belleville, M. Cantilon, G. Chetelat, M. Ewers, N. Franzmeier, G. Kempermann, W. S. Kremen, et al., “Whitepaper: Defining and investigating cognitive reserve, brain reserve, and brain maintenance,” *Alzheimer’s & Dementia*, vol. 16, no. 9, pp. 1305–1311, 2020.